Nonlin. Processes Geophys. Discuss., https://doi.org/10.5194/npg-2017-41
Manuscript under review for journal Nonlin. Processes Geophys.
Discussion started: 7 September 2017
© Author(s) 2017. CC BY 4.0 License.

Nonlinear Processes in Geophysics
Discussions
Open Access
EGU

Intermittent turbulence in the heliosheath and the magnetosheath plasmas based on Voyager and THEMIS data

Wiesław M. Macek[1,2], Anna Wawrzaszek[2], and Beata Kucharuk[1]

[1]Faculty of Mathematics and Natural Sciences, Cardinal Stefan Wyszyński University, Wóycickiego 1/3, 01-938 Warsaw, Poland
[2]Space Research Centre, Polish Academy of Science, Bartycka 18A, 00-716 Warsaw, Poland

Correspondence to: Wiesław M. Macek (macek@cbk.waw.pl)

Abstract. Turbulence is complex behavior that is ubiquitous in space, including the environments of the heliosphere and the magnetosphere. Our studies on solar wind turbulence including the heliosheath, and even at the heliospheric boundaries, also beyond the ecliptic plane, have shown that turbulence is intermittent in the entire heliosphere. As is known turbulence in space plasmas often exhibits substantial deviations from normal distributions. Therefore, we analyze the fluctuations of plasma and magnetic field parameters also in the magnetosheath behind the Earth's bow shock. In particular, based on THEMIS observations, we have already suggested that turbulence behind the quasi-perpendicular shock is more intermittent with larger kurtosis then that behind the quasi-parallel shocks. Following this study we would like to present detailed analysis of the level of intermittency in the magnetosheath depending on various characteristics of plasma behind the bow shock and now also near the magnetopause. In particular, we have verified that behind the bow shock turbulence is often more intermittent at higher Alfvénic Mach numbers than at the lower numbers. However, the level of intermittency for the outgoing waves seems to be similar as for the incoming waves, which is consistent with equipartition of energy between these oppositely propagating Alfvén waves. We hope that the difference in characteristic behavior of these fluctuations in various regions of space plasmas can help to detect some complex structures in space missions in the near future.

1 Introduction

Turbulence is complex behavior that is ubiquitous in space, including the solar wind, interplanetary, and interstellar media, as well as planetary and interstellar shocks (e.g., Bruno and Carbone, 2016). These shocks are usually collisionless and processes responsible for the plasma are substantially different from ordinary gases, see e.g. (Kivelson and Russell, 1995; Burgess and Scholer, 2015). Namely, the necessary coupling is usually provided by nonlinear structures at various scales, possibly exhibiting fractal or multifractal self-similarity properties (e.g., Burlaga, 1995; Macek, 2006). In addition, dissipation (so called quasi-viscosity) could often result from wave damping or other processes related to electric current structures. The mechanism of complexity of space and astrophysical plasmas is still a challenge to turbulence problems (Chang, 2015).

Nonlin. Processes Geophys. Discuss., https://doi.org/10.5194/npg-2017-41
Manuscript under review for journal Nonlin. Processes Geophys.
Discussion started: 7 September 2017
© Author(s) 2017. CC BY 4.0 License.

2 Multifractal Model

In our view, we should still rely on phenomenological models of intermittent turbulence, which can grasp multiplicative processes leading to complex behavior of the plasma in a simply way. As we have often argued (e.g., Macek, 2006, 2007; Macek and Wawrzaszek, 2009), the most useful concept for such a phenomenological study is a topological object namely the generalized two-scale weighted Cantor set — an example of multifractals — as described, for example, by Falconer (1990). The turbulence model based on this set is sketched here in Figure 1, as taken from Macek (2007). We see that at each step of constructing of the generalized Cantor set one needs to specify two scales l_1 and l_2 ($l_1 + l_2 \leq 1$) associated with probability measures p and $1-p$. In fact, fractals and multifractals could be considered as a convenient mathematical language useful for understanding dynamics of turbulence, as already postulated by Mandelbrot (1982). In fact, in this review we will provide some arguments that this surprisingly simple mathematical rule provides a very efficient tool for phenomenological analysis of complex turbulent media.

Moreover, for the two-scale weighted Cantor set model the singularity multifractal spectrum shown in Figure 2 can easily be calculated (e.g., Ott, 1993). In particular, the width of this universal function, Δ, is obtained analytically by the following equation

$$\Delta \equiv \alpha_{\max} - \alpha_{\min} = D_{-\infty} - D_{\infty} = \left| \frac{\log(1-p)}{\log l_2} - \frac{\log(p)}{\log l_1} \right|. \quad (1)$$

Naturally, this quantity Δ is just the difference between the maximum and minimum dimensions related to the regions in the phase space with the least dense and most dense probability densities, and hence it has been proposed by Macek (2007) and Macek and Wawrzaszek (2009) as a degree of multifractality. Moreover, since this parameter Δ exhibits a deviation from a strict self-similarity it can also be used as a degree of intermittency, as explained in (Frisch, 1995, chapter 8). One can expect that in the solar wind Δ reveals various nonlinear phenomena, including nonlinear pressure pulses related to magnetosonic waves, as argued by Burlaga et al. (2003, 2007).

The other parameter A describing the multifractal scaling, is the measure of asymmetry of the spectrum as defined by Macek and Wawrzaszek (2009)

$$A \equiv \frac{\alpha_0 - \alpha_{\min}}{\alpha_{\max} - \alpha_0}, \quad (2)$$

where $\alpha = \alpha_0$ is the point at which the spectrum has its maximum, $f(\alpha_0) = 1$. In particular, in a simpler case when $A = 1$ ($l_1 = l_2 = 0.5$) one-scale p-model is recovered (e.g., Meneveau and Sreenivasan, 1987), and for a monofractal the function in Figure 2 is reduced to a point.

In principle, for experimental time series one can recover the multifractal spectrum and fit to either well-known p model or the more general two-scale weighted Cantor set model. For Voyager data this can be done in the following way. Namely, the generalized multifractal measures $p(l)$ depending on scale l can be constructed using magnetic field strength fluctuations (Burlaga, 1995). Normalizing a time series of daily averages $B(t_i)$, where $i = 1, \ldots, N = 2^n$ for $j = 2^{n-k}$, $k = 0, 1, \ldots, n$

$$p(x_j, l) \equiv \frac{1}{N} \sum_{i=1+(j-1)\Delta t}^{j\Delta t} B(t_i) = p_j(l), \quad (3)$$

Nonlin. Processes Geophys. Discuss., https://doi.org/10.5194/npg-2017-41
Manuscript under review for journal Nonlin. Processes Geophys.
Discussion started: 7 September 2017
© Author(s) 2017. CC BY 4.0 License.

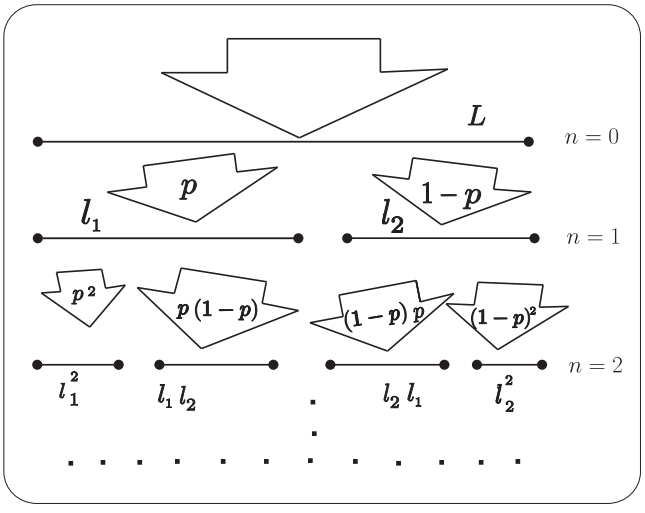

Figure 1. Two-scale weighted Cantor set model for asymmetric solar wind turbulence (Macek, 2007).

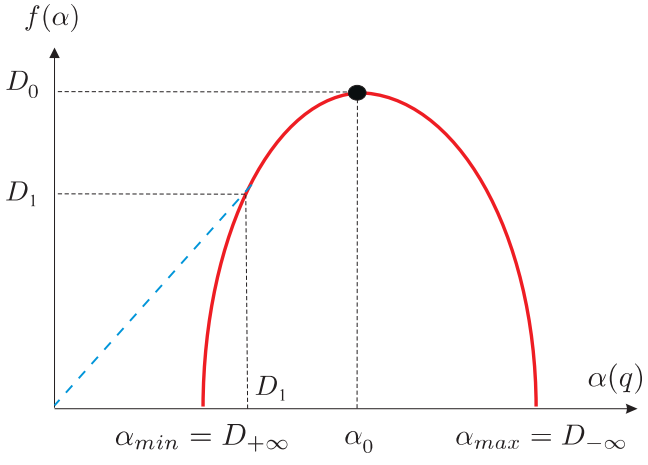

Figure 2. The singularity multifractal spectrum $f(\alpha)$ versus the singularity strength α with some general properties: (1) the maximum value of $f(\alpha)$ is D_0; (2) $f(D_1) = D_1$; and (3) the line joining the origin to the point on the $f(\alpha)$ curve, where $\alpha = D_1$ is tangent to the curve, as taken from (Ott, 1993).

Nonlin. Processes Geophys. Discuss., https://doi.org/10.5194/npg-2017-41
Manuscript under review for journal Nonlin. Processes Geophys.
Discussion started: 7 September 2017
© Author(s) 2017. CC BY 4.0 License.

Nonlinear Processes in Geophysics
Discussions
Open Access
EGU

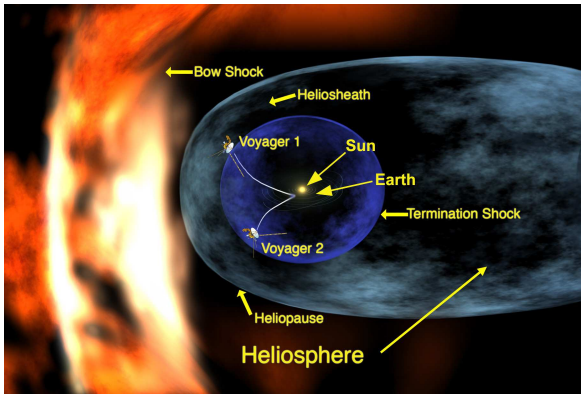

Figure 3. Schematic of the Heliospheric Boundaries [credit: NASA/Walt Feimer].

is calculated with the successive average values $\langle B(t_i, \Delta t)\rangle$ of $B(t_i)$ between t_i and $t_i + \Delta t$, for each $\Delta t = 2^k$ (Macek et al., 2011). By using Taylor's hypothesis, we can argue that $p(x_j, l)$ can be regarded as a probability that at a position $x = v_{\rm sw}t$, at time t, where $v_{\rm sw}$ is the average solar wind speed, a given magnetic flux is transferred to a spatial scale $l = v_{\rm sw}\Delta t$.

In this way Burlaga (1995) has shown that in the inertial range the average value of the qth moment of B at various scales l scales as

$$\langle B^q(l)\rangle \sim l^{\gamma(q)}, \tag{4}$$

where the exponent γ is related to the generalized dimension, $\gamma(q) = (q-1)(D_q - 1)$. Using these slopes for each real q, the values of D_q can be determined with Equation (4). Alternatively, as explained by Macek and Wawrzaszek (2009), the multifractal function $f(\alpha)$ versus scaling index α shown in Figure 2, which exhibits universality of the multifractal scaling behavior, can be obtained using the Legendre transformation. It is worth noting, however, that we obtain this multifractal universal function directly from the slopes using this direct method in various situations (see, Macek and Wawrzaszek, 2009; Macek et al., 2011, 2012, 2014).

3 Heliosheath Turbulence

The schematic of the heliospheric boundaries is shown in Figure 3.

3.1 Heliosheath Data

Voyager 1 entered the heliosheath after crossing the termination heliospheric shock at 94 AU in 2004, while Voyager 2 crossed this shock at 84 AU in 2007. The results for both spacecraft immersed in the heliosheath are presented in Figure 4, case (a) at 94–97 AU for the year 2005 and (c) at 105–107 AU for the year 2008 for Voyager 1, and Voyager 2 in case (b) at 85–88 AU for the year 2008 and (d) at 88–90 AU for the year 2009, respectively (Macek et al., 2014).

Nonlin. Processes Geophys. Discuss., https://doi.org/10.5194/npg-2017-41
Manuscript under review for journal Nonlin. Processes Geophys.
Discussion started: 7 September 2017
© Author(s) 2017. CC BY 4.0 License.

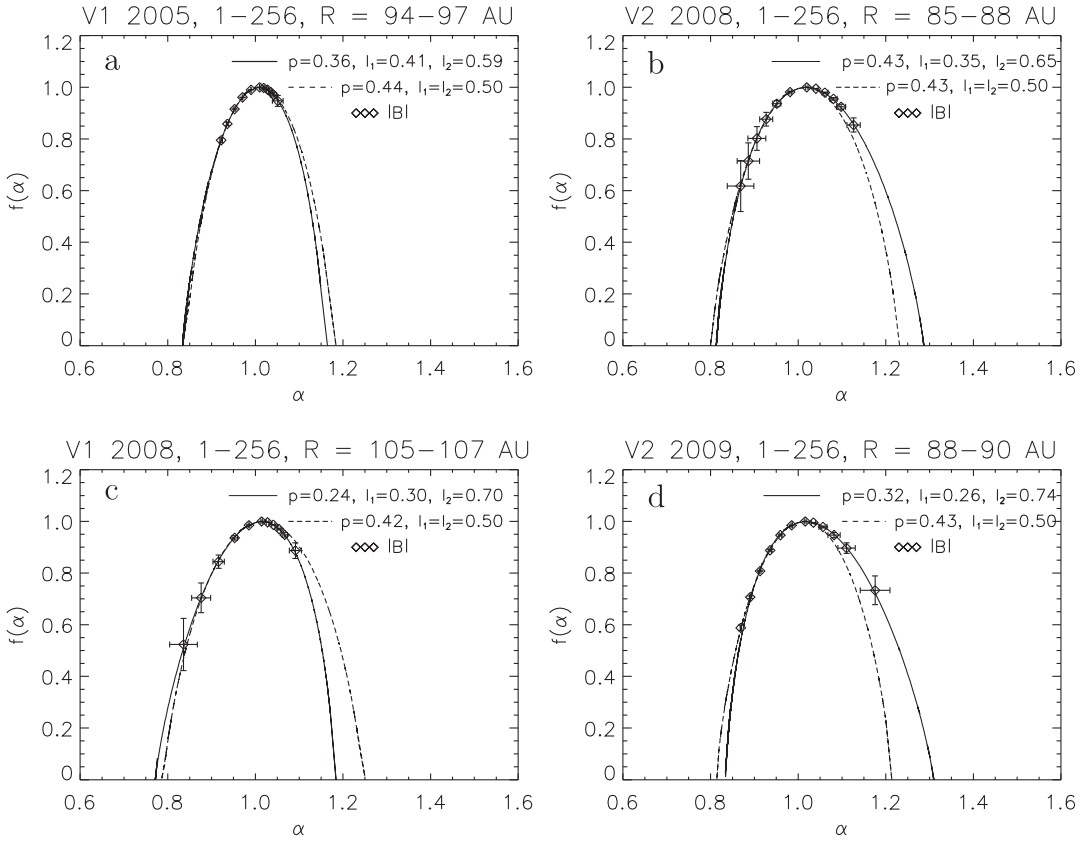

Figure 4. The singularity spectrum $f(\alpha)$ as a function of a singularity strength α. The values are calculated for the weighted two-scale (continuous lines) model and the usual one-scale (dashed lines) p-model with the parameters fitted using the magnetic fields (diamonds) measured by Voyager 1 in the heliosheath at various heliocentric distances of (a) 94–97 AU and (c) 105–107 AU AU, and Voyager 2 at (b) 85–88 AU and (d) 88–90 AU, correspondingly, taken from (Macek et al., 2014).

We have also calculated the degree of multifractality Δ, as given in Equation (1), for Voyager 1 in the heliosheath depending on the heliospheric distances during different phases of the solar cycle: minimum (MIN), maximum (MAX), declining (DEC) and rising (RIS) phases, which is now demonstrated in Figure 5 by a dashed line for two various scaling ranges from 2 to 32 days (cf. Macek et al., 2014). The crossings of the termination shock (TS) and the heliopause (HP) by Voyager 1 are indicated by vertical dashed lines. We see that in the heliosheath the degree of multifractality basically still follows the periodic dependence fitted inside the heliosphere (Macek et al., 2011, 2012). Naturally, the multifractal spectrum can be related to nonlinear Alfvén waves, associated with discontinuities or mirror mode structures due to some plasma instabilities or possibly current sheets (Borovsky, 2010; Tsurutani et al., 2011a, b) generated upstream of the termination shock, as discussed in our previous paper (Macek and Wawrzaszek, 2013).

In this way we have applied the multifractal model (Macek, 2007; Macek and Szczepaniak, 2008) to solar wind turbulence in the entire heliosphere (Szczepaniak and Macek, 2008; Macek and Wawrzaszek, 2009; Macek et al., 2011, 2012), also be-

Nonlin. Processes Geophys. Discuss., https://doi.org/10.5194/npg-2017-41
Manuscript under review for journal Nonlin. Processes Geophys.
Discussion started: 7 September 2017
© Author(s) 2017. CC BY 4.0 License.

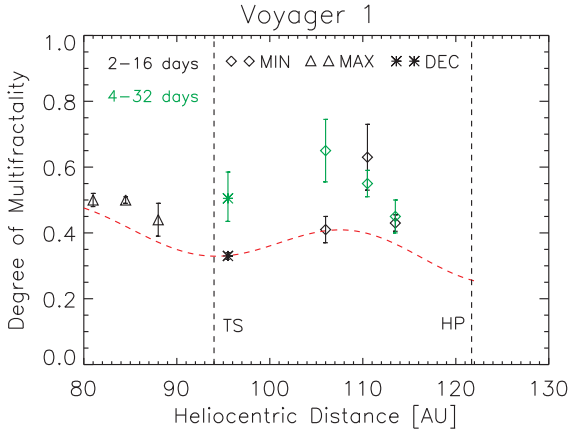

Figure 5. The parameter Δ quantifying multifractality in the heliosheath as a function of the distances from the Sun together with a periodic function shown by a continuous line during different phases of the solar cycle. The termination shock (TS) and the heliopause (HP) crossings by Voyager 1 are also indicated, taken from (Macek et al., 2014).

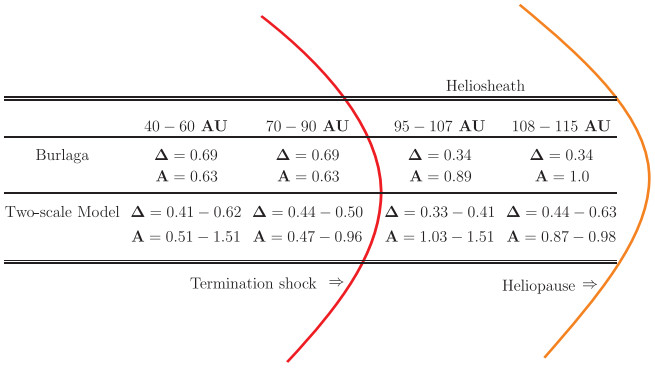

Figure 6. The degree of multifractality Δ and asymmetry A in the heliosheath as a function of the distances from the Sun. The termination shock (TS) and the heliopause (HP) crossings by Voyager 1 are also indicated (cf. Macek, 2012).

yond the ecliptic plane (Wawrzaszek and Macek, 2010; Wawrzaszek et al., 2015), and even at the heliospheric boundaries (Burlaga et al., 2013; Macek et al., 2014), and have shown that turbulence could often be intermittent. By the way, it would be difficult to argue that there is an asymmetry in these spectra for the Voyager 1 data, but there are some deviations from symmetric spectrum for Voyager 2. In summary, the values of the degree of intermittency calculated from the papers by Burlaga et al. (2006); Burlaga and Ness (2010) and our two-scale weighted Cantor set model are presented in Figure 6 (cf. Macek, 2012).

As is known turbulence in space and astrophysical plasmas exhibits deviations from normal distributions and these higher moments are often considered as signatures of intermittency. In particular, kurtosis – the fourth moment of the probability density function – is often used as a measure of intermittency (Bruno et al., 2003; Bruno and Carbone, 2013).

Nonlin. Processes Geophys. Discuss., https://doi.org/10.5194/npg-2017-41
Manuscript under review for journal Nonlin. Processes Geophys.
Discussion started: 7 September 2017
© Author(s) 2017. CC BY 4.0 License.

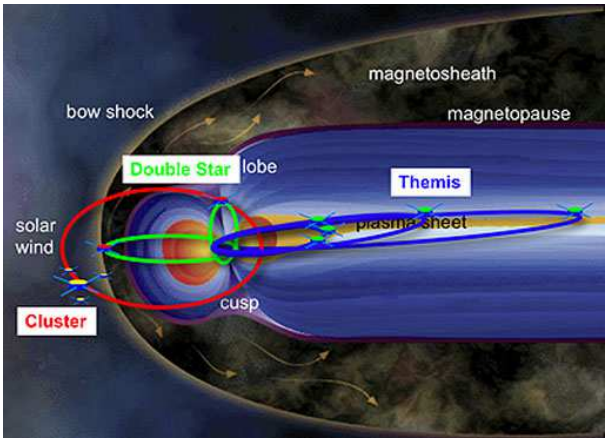

Figure 7. Schematic of THEMIS Mission [credit: NASA/ESA].

4 Magnetosheath Turbulence

Naturally, nonlinear structures responsible for turbulence have been already identified in planetary environments, also in the magnetosheath (e.g., Alexandrova, 2008; Yordanova et al., 2008). In addition, kinetic simulations by Karimabadi et al. (2014) have suggested some interesting relationships of turbulent processes near shocks to reconnection processes. But in spite of progress in MHD simulations, including Hall effects, the physical mechanisms of turbulent behavior are still not sufficiently clear.

Various space missions provide unique observational data, which help to understand phenomena in our environment in space. In particular, the THEMIS mission was launched by NASA in 2007 in order to grasp macroscale phenomena occurring during substorms (Sibeck and Angelopoulos, 2008), as schematically presented in Figure 7. In addition, for the first time THEMIS data were used for analysis of turbulence at the terrestrial bow shock. Namely, we have suggested that turbulence behind the quasi-perpendicular shock is more intermittent with larger kurtosis then that behind the quasi-parallel shocks (Macek et al., 2015).

In this review paper besides turbulence in the heliosheath, as has already been discussed in Section 3, now in Section 4 we continue our study in the entire magnetosheath also near the magnetopause. However, since it would be difficult to obtain the full multifractal spectrum using the THEMIS data, at present we only examine how the degree of multifractality resulting in deviation from the normal distribution, which is also a level of intermittency, depends on the characteristics of the solar and magnetospheric plasmas (Macek et al., 2017). The data under study are briefly described in Subsection 4.1. In Subsection 4.2 we present the results of our analysis, showing in particular that at high Alfvénic Mach numbers turbulence becomes clearly intermittent. The importance of this intermittent behavior for space plasmas is underlined in Section 5.

Nonlin. Processes Geophys. Discuss., https://doi.org/10.5194/npg-2017-41
Manuscript under review for journal Nonlin. Processes Geophys.
Discussion started: 7 September 2017
© Author(s) 2017. CC BY 4.0 License.

4.1 Magnetosheath Data

We analyze various time samples acquired during the long period between 2008 and 2015 from THEMIS mission consisting of a quintet (A, B, C, D, and E) space probes (Sibeck and Angelopoulos, 2008), as listed in Table 1. We have selected the following 29 intervals in the magnetosheath: 11 samples measured after crossing the bow shock, denoted by BS, and 18 samples obtained before leaving the magnetosheath, i.e. near magnetopause, denoted by MP. The time resolution here is 3 s and these samples taken in GSE are all (except no 11) longer than 4 h. Naturally, the length of each sample depends on the orbit of a particular probe immersed in the magnetosheath during some period of time. Please note that the time scales in the magnetosheath are much shorter than in the heliosheath.

Various characteristic plasma parameters, namely, the Alfvén Mach numbers, $M_{\rm A}$, the plasma parameter beta, β, and the magnetosonic Mach number, $M_{\rm ms}$, are calculated in the solar wind upstream: first before crossing the bow shock (before entering the magnetosheath) and next in the magnetosphere (before crossing the magnetopause). The plasma β is the ratio of the thermal pressure p to the magnetic pressure $\mathbf{B}^2/(2\mu_0\rho)$, where $\rho = mN$ is the mass density for ions of mass m and the number density N (μ_0 denotes the permeability of free space).

All these 3 plasma parameters versus sample number are depicted in Figure 8. We see that the Alfvén Mach numbers can vary substantially with the limiting value of about 25 ($5 \leq M_{\rm A} \leq 25$), and that in most cases cover β is below 5 (only 3 cases are above 10). However the magnetosonic Mach numbers are rather moderate $3.6 \leq M_{\rm ms} \leq 7.5$.

4.2 Results for the magnetosheath

Using the values of plasma and magnetic fields shown in Figures 2 and 3 of the paper by Macek et al. (2017) we can calculate the Elsässer variables, $\mathbf{z}^{\pm} = \mathbf{V} \pm \mathbf{V}_{\rm A}$, where the characteristic Alfvénic velocity is given by $\mathbf{V}_{\rm A} = \mathbf{B}/(\mu_0\rho)^{1/2}$ (Elsasser, 1950). It worth noting that the sign is taken here relative to the local average magnetic field $\mathbf{B_o}$, which certainly depends on the time scale τ responsible for turbulence as recently noted by Gerick et al. (2017). Because the time period during which this average background magnetic field is calculated, say $d\tau$, should be substantially larger than time scale of turbulence τ, we have taken d =10. Now, following our previous work on THEMIS data, the kurtosis of the increments of the magnitudes $z^{\pm} = |\mathbf{z}^{\pm}|$ of both Elsässer variables, $\delta z^{\pm}(t,\tau) = z^{\pm}(t+\tau) - z^{\pm}(t)$, can be calculated for any given scale τ, taken in units of time resolution (Macek et al., 2015).

The obtained values of kurtosis of the increments of the fluctuations of the Elsässer variables for the outgoing and ingoing Alfvénic waves, respectively z^+ and z^-, as observed by THEMIS in the magnetosheath near the bow shock (BS, red circles) and the magnetopause (MP, white triangles), versus the Alfvén Mach number (a, b), the total plasma beta β (c, d), and the magnetosonic Mach number (e, f), corresponding to Figure 8, are presented in Figure 9 for all other 29 cases listed in Table 1. The departure of the probability density functions from normal distributions and the dependence of the kurtosis on the time scale τ for the selected four cases corresponding to Figures 2 and 3 of (Macek et al., 2017), namely near the bow shock (cases a and b) and near the magnetopause (cases c and d), are illustrated in Figures 10 and 11.

Nonlin. Processes Geophys. Discuss., https://doi.org/10.5194/npg-2017-41
Manuscript under review for journal Nonlin. Processes Geophys.
Discussion started: 7 September 2017
© Author(s) 2017. CC BY 4.0 License.

Nonlinear Processes in Geophysics
Discussions
Open Access
EGU

Table 1. List of selected samples.

No.	THEMIS	Year	Location	Interval		M_A	β	M_{ms}
				Begin	End			
				mm.dd.hh.MM	mm.dd.hh.MM			
1	THC	2008	BS	06.27.18.30	06.27.23.15	14.13	2.98	7.50
2	THC	2008	BS	07.01.16.30	07.01.22.00	12.77	2.89	6.83
3	THC	2008	BS	10.08.13.45	10.08.18.45	8.77	1.44	5.87
4	THC	2008	BS	10.18.12.45	10.18.17.30	9.97	2.85	5.33
5	THB	2009	BS	06.10.16.45	06.11.02.00	11.66	3.51	5.84
6	THC	2009	BS	07.12.14.30	07.12.21.00	15.05	4.10	7.13
7	THC	2009	BS	07.31.08.30	07.31.13.30	8.43	1.79	5.30
8	THC	2009	BS	08.12.01.00	08.12.05.15	16.93	6.25	6.70
9	THC	2009	BS	08.19.17.00	08.19.22.00	6.50	1.18	4.57
10	THB	2010	BS	01.04.07.15	01.04.15.15	6.73	1.55	4.38
11	THB	2010	BS	04.13.09.30	04.13.13.15	7.15	1.05	5.20
12	THC	2008	MP	05.14.13.45	05.15.12.45	15.93	6.95	6.23
13	THD	2008	MP	09.13.15.15	09.13.22.00	22.00	12.45	6.53
14	THC	2009	MP	06.17.21.15	06.18.23.30	8.29	2.19	4.87
15	THA	2009	MP	08.22.04.15	08.22.14.00	8.98	1.45	5.98
16	THA	2009	MP	10.28.15.00	10.29.00.15	6.98	1.08	5.00
17	THA	2009	MP	11.14.15.30	11.15.02.00	6.93	1.42	4.62
18	THA	2009	MP	12.23.14.00	12.23.21.00	9.88	2.08	5.90
19	THA	2010	MP	12.01.14.30	12.01.21.00	11.75	3.16	6.13
20	THA	2010	MP	12.03.12.45	12.03.19.30	24.68	16.48	6.43
21	THE	2010	MP	12.03.13.00	12.03.20.30	21.10	11.97	6.35
22	THA	2011	MP	11.24.17.45	11.25.00.15	8.28	1.72	5.25
23	THD	2012	MP	01.08.17.00	01.08.22.00	8.97	1.32	6.13
24	THA	2012	MP	01.15.16.30	01.16.00.15	11.00	2.97	5.83
25	THD	2012	MP	01.15.16.30	01.16.00.00	10.50	2.75	5.70
26	THE	2013	MP	01.31.17.45	02.01.00.45	11.63	3.62	5.75
27	THD	2014	MP	03.13.14.00	03.13.20.00	6.17	1.57	4.00
28	THD	2015	MP	03.23.00.45	03.23.05.30	5.27	0.51	4.40
29	THE	2015	MP	03.27.21.30	03.28.07.45	7.35	1.01	3.57

Nonlin. Processes Geophys. Discuss., https://doi.org/10.5194/npg-2017-41
Manuscript under review for journal Nonlin. Processes Geophys.
Discussion started: 7 September 2017
© Author(s) 2017. CC BY 4.0 License.

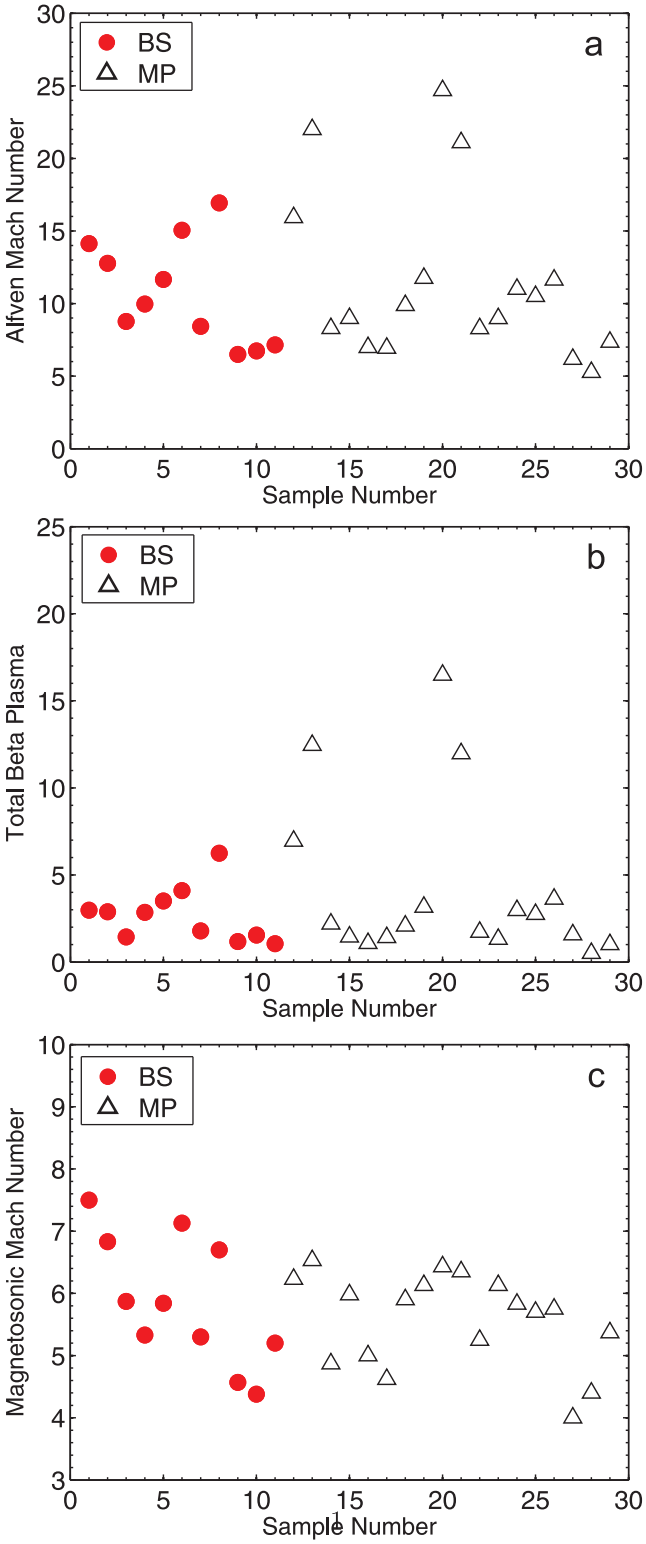

Figure 8. Alfvén Mach number (top), total plasma beta (middle) and magnetosonic Mach number (bottom) near the bow shock (BS, red circles) and the magnetopause (MP, white triangles).

Nonlin. Processes Geophys. Discuss., https://doi.org/10.5194/npg-2017-41
Manuscript under review for journal Nonlin. Processes Geophys.
Discussion started: 7 September 2017
© Author(s) 2017. CC BY 4.0 License.

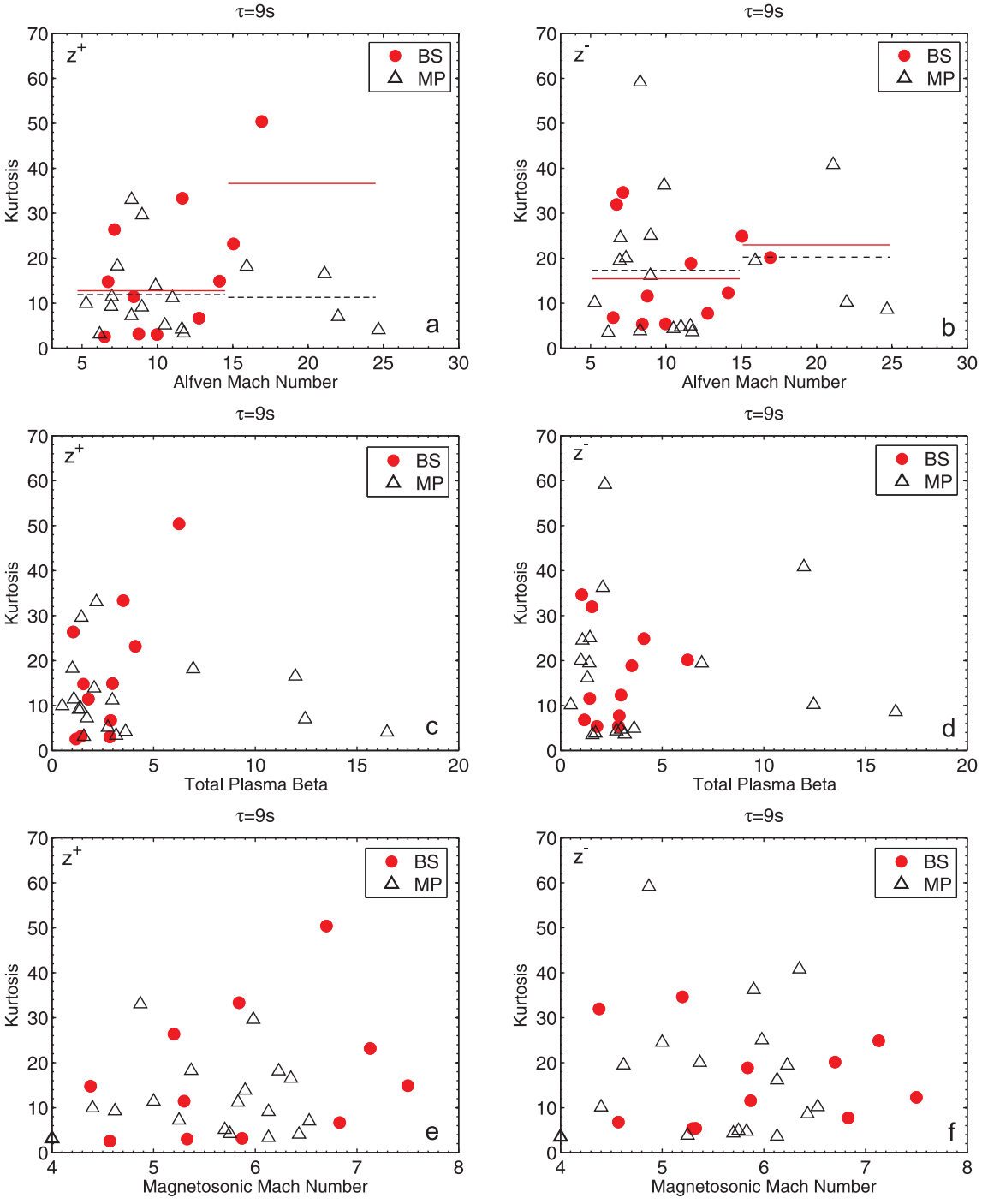

Figure 9. Kurtosis of the increments of the Elsässer variables, δz^+ and δz^-, in the magnetosheath (at scale $\tau = 9$ s) versus the Alfvén Mach number (cases a, b), with averages near the bow shock (BS, circles) marked by a continuous line and near the magnetopause (MP, triangles) by a dashed line, total plasma beta β (cases c, d), and magnetosonic Mach number (cases e, f) as observed by THEMIS for cases listed in Table 1.

Nonlin. Processes Geophys. Discuss., https://doi.org/10.5194/npg-2017-41
Manuscript under review for journal Nonlin. Processes Geophys.
Discussion started: 7 September 2017
© Author(s) 2017. CC BY 4.0 License.

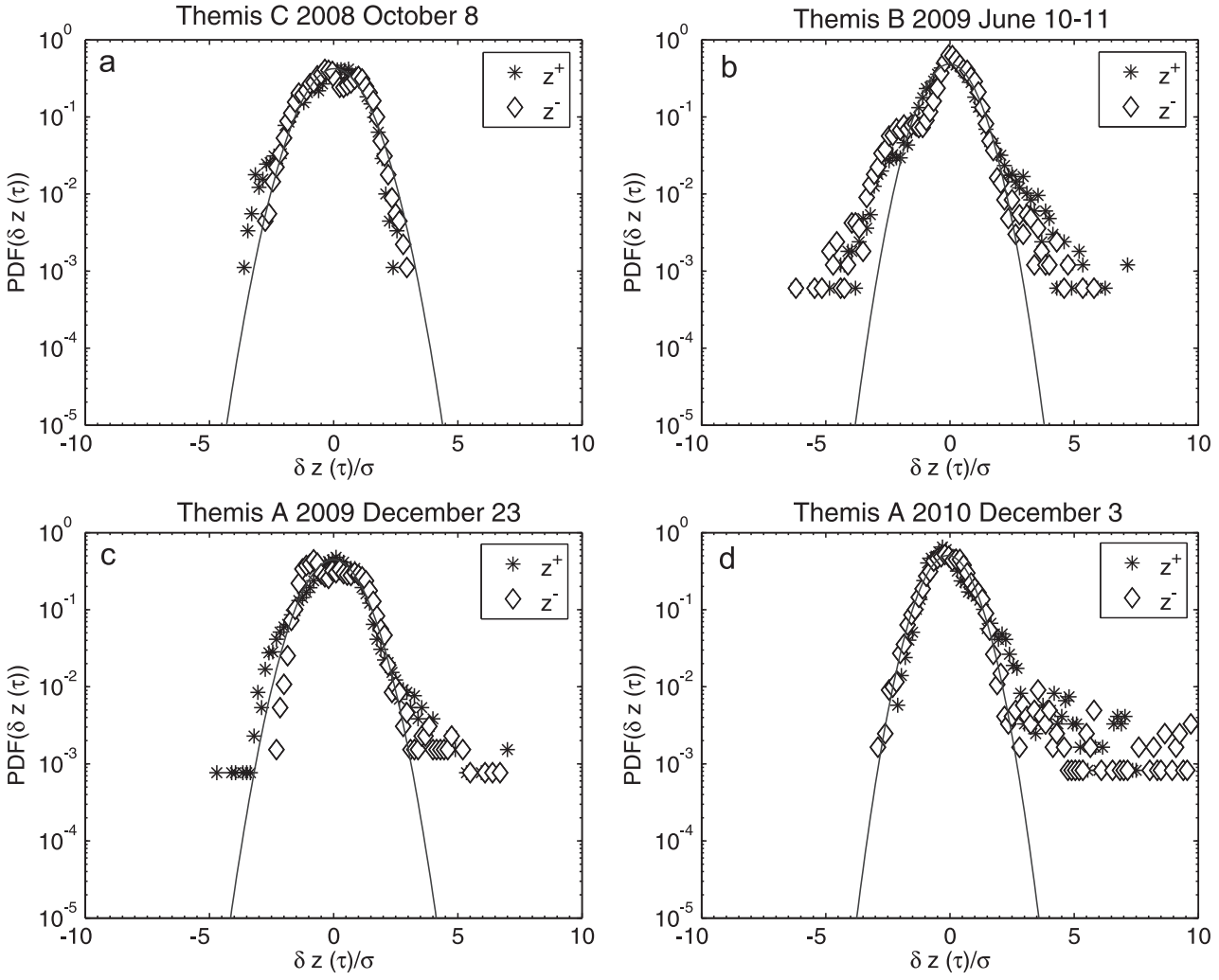

Figure 10. The probability density functions (PDF) of fluctuations of the Elsässer variables, δz^+ (stars) and δz^- (diamonds), at scales of $\tau = 9$ s, as observed by THEMIS spacecraft in the magnetosheath near the bow shock (cases a and b) and near the magnetopause (cases c and d), compared with the normal distribution (continuous lines).

Nonlin. Processes Geophys. Discuss., https://doi.org/10.5194/npg-2017-41
Manuscript under review for journal Nonlin. Processes Geophys.
Discussion started: 7 September 2017
© Author(s) 2017. CC BY 4.0 License.

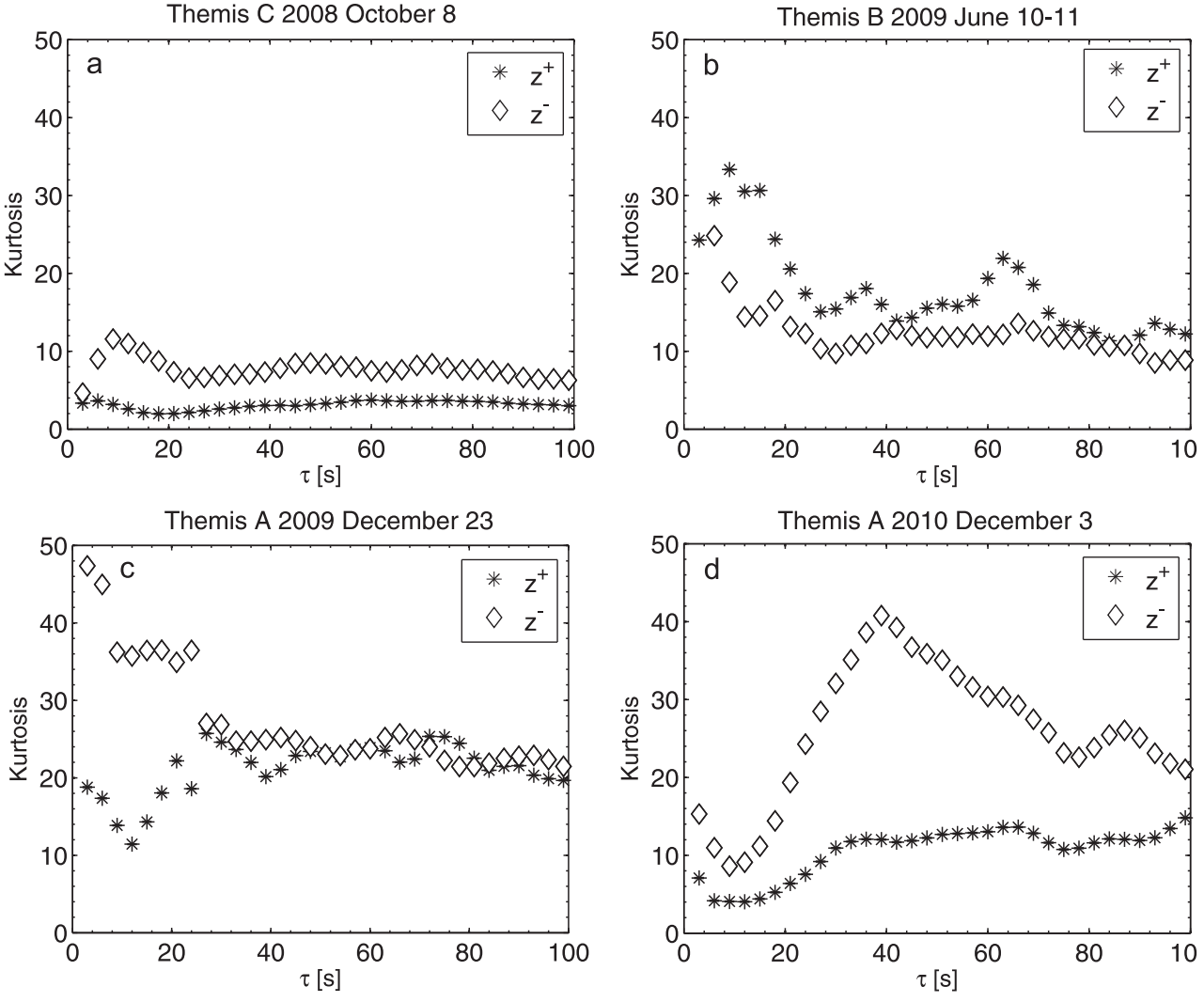

Figure 11. Kurtosis for the magnitude of the Elsässer variables, δz^+ (stars) and δz^- (diamonds), as a function of time scale τ near the bow shock (cases a and b) and near the magnetopause (cases c and d).

Nonlin. Processes Geophys. Discuss., https://doi.org/10.5194/npg-2017-41
Manuscript under review for journal Nonlin. Processes Geophys.
Discussion started: 7 September 2017
© Author(s) 2017. CC BY 4.0 License.

Nonlinear Processes in Geophysics Discussions

Figure 9 shows kurtosis for the increments of the Elsässer variables, for all the cases listed in Table 1, but for only one scale. Even though there is no clear dependence on these plasma parameters one can notice that the value of kurtosis often increases with Alfvénic Mach number. In particular, we see that for the outgoing waves, z^+, near the bow shock kurtosis increases substantially from 12.91 ± 0.06 at lower M_A (bin: $5 \leq M_A \leq 15$) to 36.78 ± 0.06 at higher M_A (bin $15 < M_A \leq 25$). However, near the magnetopause the observed change is smaller from 12.05 ± 0.05 to 11.44 ± 0.05. We have a basically similar behavior for the incoming waves, z^- (from 14.95 ± 0.06 to 22.49 ± 0.06 at BS and from 16.83 ± 0.05 to 19.76 ± 0.05 at MP).

Additionally, the selection of the four examples (illustrated in Figures 2 and 3 of (Macek et al., 2017)), cases 3, 5, 18, and 20 listed in Table 1, allows comparison of the outgoing (z^+) and incoming waves (z^-), as illustrated in Figures 10 and 11 (a), (b), (c), and (d), respectively. In Figure 10 we show the probability density functions (PDF) of fluctuations of the Elsässer variables, δz^+ and δz^-, as observed by THEMIS spacecraft in the magnetosheath at scales of $\tau = 9$ s, correspondingly, compared with the normal distribution (continuous lines), similarly as Figures 8 and 9 in the previous paper (Macek et al., 2015), but taken now a chosen scale τ of 9 s (three time the sample resolution, here 3 s). In particular, for case (a) near the bow shock kurtosis for z^+ is smaller than for z^- and the same happens for case (d) near the magnetopause for the highest value of $M_A = 25$, and high $\beta = 16.5$, where both values are somewhat larger, but for cases (b) and (c) they are rather similar.

Even though there is no clear regularity in Figure 11 showing dependence of the kurtosis on scale τ, it seems that kurtosis near the bow shock (cases a and b) is rather similar to that near the magnetopause (cases c and d). Namely, based on Figures 9 it seems that near the bow shock (circles) the intermittency seems to increase with the Alfvénic Mach number M_A and decrease with the plasma beta β near the magnetopause (triangles). We also see some difference between z^+ and z^- (Figure 11 d) for MP, especially for small scales (Figure 11 c), and therefore could consider the other cases as well, but generally speaking, the level of intermittency for the outgoing waves z^+ is usually similar as for the incoming waves z^-, which exhibits equipartition of energy between these oppositely propagating Alfvén waves.

5 Conclusions

Using our weighted two-scale Cantor set model, which is a convenient tool to investigate the asymmetry of the multifractal spectrum, we confirm the characteristic shape of the universal multifractal singularity spectrum. In fact, as seen in Figure 4, $f(\alpha)$ is a downward concave function of scaling indices α. We show that the degree of multifractality for magnetic field fluctuations of the solar wind falls steadily with the distance from the Sun. Moreover, we have considered the multifractal spectra of fluctuations of the interplanetary magnetic field strength before and after crossing of the heliospheric termination shock by Voyager 1 and 2 near 94 and 84 AU from the Sun, correspondingly.

Further, we have provided an important evidence that the large-scale magnetic field fluctuations reveal the multifractal structure not only in the outer heliosphere, but in the entire heliosheath, even near the heliopause. Naturally, the evolution of the multifractal distributions should be related to some physical (MHD) models, as suggested by Burlaga et al. (2003, 2007). The driver of the multifractality in the heliosheath could be the solar variability on scales from hours to days, fast and slow streams or shocks interactions, and other nonlinear structures discussed by Macek and Wawrzaszek (2013). In our view, any

© Author(s) 2017. CC BY 4.0 License.

accurate physical model must reproduce the multifractal spectra. In particular, the observed non-multifractal scaling after the heliopause crossing suggest a non-intermittent behavior in the nearby interstellar medium, consistent with the smoothly varying interstellar magnetic field reported by Burlaga and Ness (2014). We have identified the scaling region of fluctuations of the interplanetary magnetic field.

In fact, using our two-scale model based on the weighted Cantor set, we have examined the universal multifractal spectra before and after crossing by Voyager 1 the termination shock at 94 AU and before crossing the heliopause at distances of about 122 AU from the Sun. Moreover, inside the heliosphere we observe the asymmetric spectrum, which becomes more symmetric in the heliosheath. We confirm that multifractality of magnetic field fluctuations embedded the solar wind plasma for large scales decreases slowly with the heliospheric distance, demonstrating that this quantity is still modulated by the solar cycles further in the heliosheath, and even in the vicinity of the heliopause, possibly approaching a uniform non-intermittent behavior in the nearby interstellar medium. We propose this change of behavior as a signature of the expected crossing of the heliopause by Voyager 2 in the near future.

Regarding the magnetosheath we have shown that turbulence for small scales is intermittent in the entire magnetosheath, in regions near the bow shock and even near the magnetopause. In particular, we have verified that at higher Alfvénic Mach numbers M_{A} fluctuations are often somewhat more intermittent than at the lower numbers, especially behind the bow shock. On the other hand, near the magnetopause intermittency becomes sometimes weaker with the increasing total plasma beta β. However, the level of intermittency for the outgoing waves (z^+) seems to be similar as for the incoming waves (z^-). In view of the space investigation in the near future, including THOR mission (e.g. Vaivads et al., 2016), we expect that the difference in characteristic behavior of these fluctuations in various regions of the magnetosheath can help to identify some new complex structures in space plasmas.

Acknowledgements. We would like to thank the magnetic field instruments team of Voyager mission, the NASA National Space Science Data Center and the Space Science Data Facility for providing Voyager data. The research leading to these results has received funding from the THEMIS project during a visit of W.M.M. at the NASA Goddard Space Flight Center. We would like to thank the plasma and magnetic field instruments team of THEMIS mission for providing the data, which are available on-line from http://cdaweb.gsfc.nasa.gov. This work has been supported by the National Science Center, Poland (NCN), through grant 2014/15/B/ST9/04782.

© Author(s) 2017. CC BY 4.0 License.

References

Alexandrova, O.: Solar wind vs magnetosheath turbulence and Alfvén vortices, Nonlin. Processes Geophys., 15, 95–108, https://doi.org/10.5194/npg-15-95-2008, http://www.nonlin-processes-geophys.net/15/95/2008/, 2008.

Borovsky, J. E.: Contribution of strong discontinuities to the power spectrum of the solar wind, Phys. Rev. Lett., 105, 111 102, https://doi.org/10.1103/PhysRevLett.105.111102, http://link.aps.org/doi/10.1103/PhysRevLett.105.111102, 2010.

Bruno, R. and Carbone, V.: The solar wind as a turbulence laboratory, Living Rev. Sol. Phys., 10, 2, https://doi.org/10.12942/lrsp-2013-2, 2013.

Bruno, R. and Carbone, V.: Turbulence in the Solar Wind, Lecture Notes in Physics, Springer International Publishing, https://books.google.pl/books?id=auo4DQAAQBAJ, 2016.

Bruno, R., Carbone, V., Sorriso-Valvo, L., and Bavassano, B.: Radial evolution of solar wind intermittency in the inner heliosphere, J. Geophys. Res., 108, 1130, https://doi.org/10.1029/2002JA009615, 2003.

Burgess, D. and Scholer, M.: Collisionless Shocks in Space Plasmas, Cambridge University Press, 2015.

Burlaga, L. F.: Interplanetary Magnetohydrodynamics, New York: Oxford University Press, 1995.

Burlaga, L. F. and Ness, N. F.: Sectors and large-scale magnetic field strength fluctuations in the heliosheath near 110 AU: Voyager 1, 2009, Astrophys. J., 725, 1306–1316, https://doi.org/10.1088/0004-637X/725/1/1306, 2010.

Burlaga, L. F. and Ness, N. F.: Voyager 1 observations of the interstellar magnetic field and the transition from the heliosheath, Astrophys. J., 784, 146, https://doi.org/10.1088/0004-637X/784/2/146, 2014.

Burlaga, L. F., Wang, C., and Ness, N. F.: A model and observations of the multifractal spectrum of the heliospheric magnetic field strength fluctuations near 40 AU, Geophys. Res. Lett., 30, 1543, https://doi.org/10.1029/2003GL016903, 2003.

Burlaga, L. F., Ness, N. F., and Acuña, M. H.: Multiscale structure of magnetic fields in the heliosheath, J. Geophys. Res., 111, A09112, https://doi.org/10.1029/2006JA011850, 2006.

Burlaga, L. F., F-Viñas, A., and Wang, C.: Tsallis distributions of magnetic field strength variations in the heliosphere: 5 to 90 AU, J. Geophys. Res., 112, A07206, https://doi.org/10.1029/2006JA012213, 2007.

Burlaga, L. F., Ness, N. F., and Stone, E. C.: Magnetic Field Observations as Voyager 1 Entered the Heliosheath Depletion Region, Science, 341, 147–150, https://doi.org/10.1126/science.1235451, http://www.sciencemag.org/content/341/6142/147.abstract, 2013.

Chang, T. T. S.: An Introduction to Space Plasma Complexity, Cambridge University Press, 2015.

Elsasser, W. M.: The hydromagnetic equations, Phys. Rev., 79, 183–183, https://doi.org/10.1103/PhysRev.79.183, 1950.

Falconer, K.: Fractal Geometry: Mathematical Foundations and Applications, J. Wiley: New York, 1990.

Frisch, U.: Turbulence. The legacy of A.N. Kolmogorov, Cambridge: Cambridge Univ. Press, 1995.

Gerick, F., Saur, J., and von Papen, M.: The uncertainty of local background magnetic field orientation in anisotropic plasma turbulence, Astrophys. J., 843, 5, http://stacks.iop.org/0004-637X/843/i=1/a=5, 2017.

Karimabadi, H., Roytershteyn, V., Vu, H. X., Omelchenko, Y. A., Scudder, J., Daughton, W., Dimmock, A., Nykyri, K., Wan, M., Sibeck, D., Tatineni, M., Majumdar, A., Loring, B., and Geveci, B.: The link between shocks, turbulence, and magnetic reconnection in collisionless plasmas, Physics of Plasmas, 21, 062308, https://doi.org/10.1063/1.4882875, 2014.

Kivelson, M. G. and Russell, C. T.: Introduction to Space Physics, Cambridge University Press, 1995.

Macek, W. M.: Modeling multifractality of the solar wind, Space Sci. Rev., 122, 329–337, https://doi.org/10.1007/s11214-006-8185-z, 2006.

Macek, W. M.: Multifractality and intermittency in the solar wind, Nonlin. Processes Geophys., 14, 695–700, 2007.

© Author(s) 2017. CC BY 4.0 License.

Macek, W. M.: Multifractal Turbulence in the Heliosphere, in: Exploring the Solar Wind, edited by Lazar, M., pp. 143–168, Intech: Croatia, 2012.

Macek, W. M. and Szczepaniak, A.: Generalized two-scale weighted Cantor set model for solar wind turbulence, Geophys. Res. Lett., 35, L02108, https://doi.org/10.1029/2007GL032263, 2008.

Macek, W. M. and Wawrzaszek, A.: Evolution of asymmetric multifractal scaling of solar wind turbulence in the outer heliosphere, J. Geophys. Res., 114, A03108, https://doi.org/10.1029/2008JA013795, 2009.

Macek, W. M. and Wawrzaszek, A.: Voyager 2 observation of the multifractal spectrum in the heliosphere and the heliosheath, Nonlinear Processes Geophys., 20, 1061–1070, https://doi.org/10.5194/npg-20-1061-2013, http://www.nonlin-processes-geophys.net/18/287/2011/, 2013.

Macek, W. M., Wawrzaszek, A., and Carbone, V.: Observation of the multifractal spectrum at the termination shock by Voyager 1, Geophys. Res. Lett., 38, L19 103, https://doi.org/10.1029/2011GL049261, 2011.

Macek, W. M., Wawrzaszek, A., and Carbone, V.: Observation of the multifractal spectrum in the heliosphere and the heliosheath by Voyager 1 and 2, J. Geophys. Res., 117, A12101, https://doi.org/10.1029/2012JA018129, 2012.

Macek, W. M., Wawrzaszek, A., and Burlaga, L. F.: Multifractal structures detected by Voyager 1 at the heliospheric boundaries, Astrophys. J. Lett., 793, L30, https://doi.org/10.1088/2041-8205/793/2/L30, 2014.

Macek, W. M., Wawrzaszek, A., and Sibeck, D. G.: THEMIS observation of intermittent turbulence behind the quasi-parallel and quasi-perpendicular shocks, J. Geophys. Res., 120, 7466–7476, https://doi.org/10.1002/2015JA021656, 2015.

Macek, W. M., Wawrzaszek, A., Kucharuk, B., and Sibeck, D. G.: THEMIS observation of intermittent ansotropic turbulence in the magnetosheath, J. Geophys. Res., submitted, 2017.

Mandelbrot, B. B.: The Fractal Geometry of Nature, W. H. Freeman and Company, San Francisco, 1982.

Meneveau, C. and Sreenivasan, K. R.: Simple multifractal cascade model for fully developed turbulence, Phys. Rev. Lett., 59, 1424–1427, https://doi.org/10.1103/PhysRevLett.59.1424, 1987.

Ott, E.: Chaos in Dynamical Systems, Cambridge: Cambridge Univ. Press, 1993.

Sibeck, D. G. and Angelopoulos, V.: THEMIS science objectives and mission phases, Space Sci. Rev., 141, 35–59, https://doi.org/10.1007/s11214-008-9393-5, 2008.

Szczepaniak, A. and Macek, W. M.: Asymmetric multifractal model for solar wind intermittent turbulence, Nonlin. Processes Geophys., 15, 615–620, 2008.

Tsurutani, B. T., Echer, E., Verkhoglyadova, O. P., Lakhina, G. S., and Guarnieri, F. L.: Mirror instability upstream of the termination shock (TS) and in the heliosheath, J. Atmospheric Solar-Terrestrial Phys., 2011a.

Tsurutani, B. T., Lakhina, G. S., Verkhoglyadova, O. P., Echer, E., Guarnieri, F. L., Narita, Y., and Constantinescu, D. O.: Magnetosheath and heliosheath mirror mode structures, interplanetary magnetic decreases, and linear magnetic decreases: Differences and distinguishing features, J. Geophys. Res., 2011b.

Vaivads, A., Retinò, A., Soucek, J., Khotyaintsev, Y. V., Valentini, F., Escoubet, C. P., Alexandrova, O., André, M., Bale, S. D., Balikhin, M., Burgess, D., Camporeale, E., Caprioli, D., Chen, C. H. K., Clacey, E., Cully, C. M., de Keyser, J., Eastwood, J. P., Fazakerley, A. N., Eriksson, S., Goldstein, M. L., Graham, D. B., Haaland, S., Hoshino, M., Ji, H., Karimabadi, H., Kucharek, H., Lavraud, B., Marcucci, F., Matthaeus, W. H., Moore, T. E., Nakamura, R., Narita, Y., Nemecek, Z., Norgren, C., Opgenoorth, H., Palmroth, M., Perrone, D., Pinçon, J.-L., Rathsman, P., Rothkaehl, H., Sahraoui, F., Servidio, S., Sorriso-Valvo, L., Vainio, R., Vörös, Z., and

© Author(s) 2017. CC BY 4.0 License.

Wimmer-Schweingruber, R. F.: Turbulence Heating ObserveR - satellite mission proposal, Journal of Plasma Physics, 82, 905820501, https://doi.org/10.1017/S0022377816000775, 2016.

Wawrzaszek, A. and Macek, W. M.: Observation of the multifractal spectrum in solar wind turbulence by Ulysses at high latitudes, J. Geophys. Res., 115, A07104, https://doi.org/10.1029/2009JA015176, 2010.

Wawrzaszek, A., Echim, M., Macek, W. M., and Bruno, R.: Evolution of intermittency in the slow and fast solar wind beyond the ecliptic plane, Astrophys. J. Lett., 814, L19, https://doi.org/10.1088/2041-8205/814/2/L19, 2015.

Yordanova, E., Vaivads, A., André, M., Buchert, S. C., and Vörös, Z.: Magnetosheath plasma turbulence and its spatiotemporal evolution as observed by the Cluster spacecraft, Phys. Rev. Lett., 100, 205003, https://doi.org/10.1103/PhysRevLett.100.205003, 2008.